JB
Journals.ASM.org

How *Escherichia coli* Tolerates Profuse Hydrogen Peroxide Formation by a Catabolic Pathway

Sripriya Ravindra Kumar,* James A. Imlay

Department of Microbiology, University of Illinois, Urbana, Illinois, USA

When *Escherichia coli* grows on conventional substrates, it continuously generates 10 to 15 μM/s intracellular H_2O_2 through the accidental autoxidation of redox enzymes. Dosimetric analyses indicate that scavenging enzymes barely keep this H_2O_2 below toxic levels. Therefore, it seemed potentially problematic that *E. coli* can synthesize a catabolic phenylethylamine oxidase that stoichiometrically generates H_2O_2. This study was undertaken to understand how *E. coli* tolerates the oxidative stress that must ensue. Measurements indicated that phenylethylamine-fed cells generate H_2O_2 at 30 times the rate of glucose-fed cells. Two tolerance mechanisms were identified. First, in enclosed laboratory cultures, growth on phenylethylamine triggered induction of the OxyR H_2O_2 stress response. Null mutants (Δ*oxyR*) that could not induce that response were unable to grow. This is the first demonstration that OxyR plays a role in protecting cells against endogenous H_2O_2. The critical element of the OxyR response was the induction of H_2O_2 scavenging enzymes, since mutants that lacked NADH peroxidase (Ahp) grew poorly, and those that additionally lacked catalase did not grow at all. Other OxyR-controlled genes were expendable. Second, phenylethylamine oxidase is an unusual catabolic enzyme in that it is localized in the periplasm. Calculations showed that when cells grow in an open environment, virtually all of the oxidase-generated H_2O_2 will diffuse across the outer membrane and be lost to the external world, rather than enter the cytoplasm where H_2O_2-sensitive enzymes are located. In this respect, the periplasmic compartmentalization of phenylethylamine oxidase serves the same purpose as the peroxisomal compartmentalization of oxidases in eukaryotic cells.

Hydrogen peroxide (H_2O_2) is a toxic oxidant that is formed inside all aerobic organisms. Studies with *Escherichia coli* have determined that H_2O_2 arises inside this model organism at a rate of 10 to 15 μM/s during growth in air-saturated glucose medium (1). Like virtually all forms of life, *E. coli* protects itself from this endogenous H_2O_2 through the combined actions of peroxidases and catalases, which rapidly degrade it. When mutants that lack these enzymes are moved from anoxic to oxic media, they quickly accumulate ~1 μM intracellular H_2O_2, which creates critical biosynthetic and catabolic defects by damaging iron-sulfur and mononuclear iron enzymes (2–4). These mutants also exhibit high rates of mutagenesis from oxidative DNA damage (5).

The endogenous H_2O_2 is generated in two ways: by the adventitious oxidation of redox enzymes and through the turnover of committed oxidases. Adventitious enzyme oxidation occurs when oxygen collides with the reduced cofactors of redox enzymes whose purpose is to transfer electrons from one organic molecule to another (6). The collision precipitates accidental electron transfers to oxygen instead, generating a mixture of superoxide and H_2O_2. Flavoproteins are especially vulnerable to these reactions; NADH dehydrogenase II, sulfite reductase, lipoamide dehydrogenase, and fumarate reductase all exhibit this behavior (7–9). Oxygen intercepts only about 1% of the electrons that flow through these enzymes; however, these enzymes belong to major pathways, so their fluxes are high enough that they collectively produce substantial H_2O_2. In glucose-grown cells, such reactions are apparently the predominant sources of H_2O_2, since the rate of intracellular H_2O_2 formation depends upon the concentration of dissolved oxygen (1). This dependency matches the autoxidation behavior of these enzymes, which similarly generate H_2O_2 in proportion to oxygen concentration *in vitro*, but not that of oxidases, whose turnover rate becomes saturated at low levels of oxygen.

Nevertheless, *E. coli* does contain several oxidases that generate H_2O_2 as a stoichiometric reaction product. Their contributions toward endogenous H_2O_2 production are typically small because they belong to low-flux pathways. Suspected examples include protoporphyrinogen oxidase and pyridoxine 5′-phosphate oxidase, which are requisite for heme synthesis and pyridoxamine salvage. An exception is aspartate oxidase, which catalyzes the committed step in nicotinamide formation. Nicotinamide cofactors are far more abundant (ca. 2 mM) than are heme or pyridoxamine cofactors, so the biosynthetic pathway processes about 3 μM substrate/s. The H_2O_2 thereby formed by aspartate oxidase contributes about 25% of the endogenous H_2O_2 in *E. coli* (10).

In aerobic *E. coli*, the threat posed by endogenous reactive oxygen species is narrowly balanced by the titers of scavenging enzymes. The primary scavenger of H_2O_2 is an NADH peroxidase (also known as Ahp), which is present at ca. 5 μM inside exponentially growing cells (11, 12). Through the combination of its extreme abundance and its high catalytic efficiency, Ahp is estimated to keep the steady-state concentration of H_2O_2 at only 50 nM, about 30 molecules per cell (13). This high scavenging activity is absolutely necessary: H_2O_2 reacts very rapidly with vulnerable enzymes, and with 50 nM H_2O_2 in the cytoplasm the half-time for

Received 25 June 2013 Accepted 27 July 2013
Published ahead of print 2 August 2013
Address correspondence to James A. Imlay, jimlay@illinois.edu.
* Present address: Sripriya Ravindra Kumar, California Institute of Technology, Division of Biology, Pasadena, California, USA.
Supplemental material for this article may be found at http://dx.doi.org/10.1128/JB.00737-13.

doi:10.1128/JB.00737-13

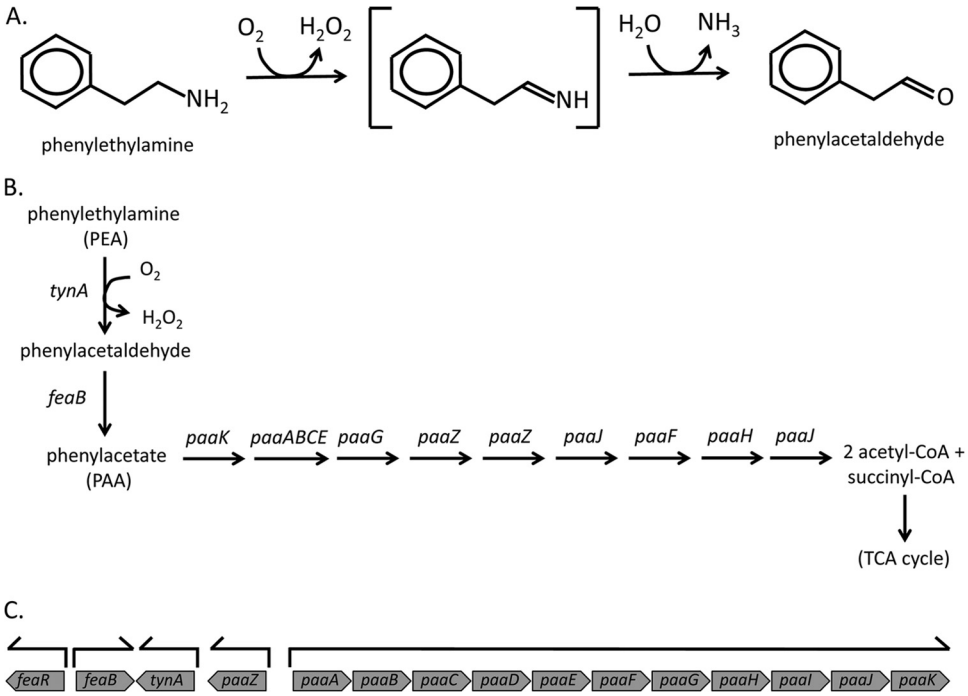

FIG 1 Catabolic pathway for phenylethylamine. (A) The phenylethylamine oxidase reaction catalyzed by Cu-MAO. The imine intermediate (center) is conjugated to topaquinone (53). (B) The catabolic pathway. Cu-MAO is encoded by *tynA*. CoA, coenzyme A. (C) Arrangement of relevant genes on the *E. coli* chromosome. The *feaR* gene encodes a positive regulator of *tynA* (64).

the damage of vulnerable enzymes is estimated to be only about 30 min. If the H_2O_2 concentration were allowed to rise much higher, these enzymes would quickly lose activity and the pathways to which they belong would cease to function.

Therefore, it is striking that *E. coli* K-12 strains have one enzyme that could generate H_2O_2 at a very substantial rate: a copper-dependent monoamine oxidase (Cu-MAO). Enzymes of the MAO class catalyze the conversion of primary amines to aldehydes, with the consumption of molecular oxygen and the release of ammonia and H_2O_2 (Fig. 1A). Monoamine oxidases lack specificity, and Cu-MAO of *E. coli* can act upon dopamine, tyramine, and 3-nitrotyramine (14). However, a primary physiological role appears to be the catabolism of phenylethylamine, which accrues in natural habitats when other bacteria decarboxylate phenylalanine (15–18). The enzyme exhibits high specificity for phenylethylamine (K_m, 1 μM; k_{cat}/K_m, $1.6 \times 10^7\ M^{-1}\ s^{-1}$) (19); its structural gene sits adjacent to an operon that encodes a pathway to degrade phenylacetate, the product of Cu-MAO action upon phenylethylamine (Fig. 1B) (20–22); and it is specifically induced when phenylethylamine (PEA) is provided as a carbon source (20). The fact that Crp regulates this pathway (23, 24) indicates that it serves a catabolic role rather than exclusively one of detoxification. Indeed, it has been shown that the pathway can enable *E. coli* to grow using PEA as the sole carbon source (20). The yield of H_2O_2 might be expected to be commensurately large. The following question then arises: does the H_2O_2 released by the Cu-MAO create unusual cellular stress?

The Cu-MAO is localized in the *E. coli* periplasm (25), and this compartmentalization might reduce the amount of H_2O_2 that enters the cytoplasm, where the known H_2O_2-sensitive enzymes reside. Alternatively, the OxyR stress response to H_2O_2 (26) might help the cell to cope with the stress that the enzyme creates. The OxyR response triggers the further induction of Ahp and catalase, the suppression of DNA damage through sequestration of intracellular iron, and the protection of mononuclear iron and iron-sulfur enzymes by the induction of manganese import and an alternative pathway of cluster assembly (27–32). The OxyR regulon has been regarded as a defense against H_2O_2 from environmental sources, but it might play a role in defending the cell against endogenous H_2O_2 if the flux from Cu-MAO is high. The aim of this study was to quantify the flux through Cu-MAO, to test whether the H_2O_2 it releases creates unusual stress inside the cell, and to appraise whether OxyR-dependent defenses are engaged when Cu-MAO is active.

MATERIALS AND METHODS

Chemicals. 2-Phenylethylamine hydrochloride, 2-phenylacetic acid, 2-phenylacetaldehyde, hydrogen peroxide, ferrous ammonium sulfate, β-mercaptoethanol, calcium chloride, copper sulfate, *o*-nitrophenyl-β-D-galactopyranoside, sodium dodecyl sulfate, and L-amino acids were purchased from Sigma-Aldrich. Dimethyl sulfoxide, potassium nitrate, ammonium sulfate, sodium citrate, glucose, and Tris-HCl were from Fisher; bovine serum albumin (BSA) and Coomassie protein reagent were from Pierce. Catalase was purchased from Worthington, Tris-borate EDTA from Meditech, and 2,4-dinitrophenylhydrazine from Fluka. PuRe *Taq* ready-to-go PCR beads were from GE Healthcare. Water used to prepare buffers was purified using a Labconco Water Pro PS system with deionized water as the feedstock.

Growth medium. Derivatives of M63 medium comprised the defined medium used in this study. M63 medium (33) consisted of minimal 63 salts [0.1 M KH_2PO_4, 10 mM $(NH_4)_2SO_4$, 1 μg/ml $Fe(NH_4)_2(SO_4)_2$, and 0.5 mM $MgSO_4 \cdot 7H_2O$, pH 7.0]. Ten mM 2-phenylethylamine hydrochloride (PEA), 10 mM 2-phenylacetic acid (PAA), or 0.7% glycerol was

used as the carbon source. Six noncatabolizable amino acids (Lys, Val, Ile, Leu, His, and Met) were routinely supplemented at 0.25 mM concentration. When PEA was tested as the sole nitrogen source, both the ammonium sulfate and the amino acids were omitted from the medium. In experiments involving Hpx$^-$ mutants (Δ*ahpCF* Δ*katG* Δ*katE*) (11), 0.25 mM Phe, Trp, and Tyr were added to circumvent the aromatic auxotrophy imposed by unscavenged H_2O_2. When glycerol was used as a carbon source under anaerobic conditions, 20 mM potassium nitrate was added as a terminal electron acceptor. LB medium contained (per liter) 10 g Bacto tryptone (Difco), 5 g yeast extract (Difco), and 10 g sodium chloride (33).

To prepare a medium for anaerobic cultures, the medium was first degassed by filtering/autoclaving. It was then moved into a Coy anaerobic chamber. After about 36 to 48 h, the medium was sufficiently anaerobic for use.

Growth conditions. Liquid cultures were routinely grown in M63 medium at 30°C. Aerobic cultures were grown in shaking flasks, and anaerobic cultures were grown in a Coy chamber (Coy Laboratory Products, Inc.) at 37°C under 85% N_2, 10% H_2, and 5% CO_2. The optical densities of all cultures were measured at 600 nm (OD_{600}).

The permanent stocks of strains that were stored at −80°C were first streaked on LB solid medium and incubated overnight. The colonies from this LB plate were streaked on different solid minimal media. Colonies appeared overnight on glucose plates, after 48 h on glycerol plates, between 48 and 72 h on PEA plates, and between 72 and 96 h on PAA plates. Unless otherwise indicated, growth in PEA or PAA medium was initiated by inoculation from a plate of the same composition.

Strains. The strains that were used in this study are listed in Table S1 in the supplemental material. They were derived from *E. coli* K-12. Most studies were conducted on strains derived from W3110. Note that standard *E. coli* strains varied in their ability to catabolize PEA (see Discussion).

The Δ*dsbG* mutant strain was constructed by Red/Gam-mediated recombination (34) using the primers 5′-ACTGACTGAAAAGGACAAATTAATG-3′ (forward) and 5′-AGCAGGGATATAGTTCAACCATCCATGAATTACCTT-3′ (reverse) to knock out 744 bp. The *ahpC′-lacZ* transcriptional fusion was constructed using CRIM plasmids (35). The *ahpC* promoter (296 bp) was inserted into pSJ501 (a plasmid with the *lacZ* gene) at SphI and KpnI sites, resulting in pSK01. The insert was then amplified using primers 5′-CTTGCATGCTGCGGTGATTGCCCTTTGTTTATGAGGGTG-3′ (forward) and 5′-CTTGGTACCCATCTATACTTCCTCCGTGT-3′ (reverse). The *degP′-lacZ* transcriptional fusion was constructed by inserting the *degP* promoter (283 bp) insert into pSJ501 at SphI and KpnI sites, resulting in pSK02. The insert was amplified using primers 5′-CTTGCATGCCGAGGCTGTCAGTAAATTAC-3′ (forward) and 5′-CGCGGTACCCATGTATTTCAGTCTCGATTAACAG-3′ (reverse). pSJ501 is the same as pAH125, except that pSJ501 has a *cat* gene instead of a *kan* gene. The *cat* gene could be flipped out by pCP20. The constructed plasmids were transformed into the W3110/pINT-ts strain (SRK55). pINT-ts is a helper plasmid that integrates the lambda *att* of pSK01 into the *attB* site of the bacterial strain. The transformant was made to lose the helper plasmid, and they were screened to ensure they had inherited a single copy of the integrant. Note that the insertion of fusions into the *attB* site allows the native genes to remain intact.

The functionality of the *ahpC′-lacZ* fusion was confirmed by introduction of the *oxyR2* constitutive plasmid pGS058 (36), followed by assay of β-galactosidase activity. Because the *ahpC′-lacZ* fusion was initially linked to a *cam* cassette, pCP20 was used to excise the drug marker. The OxyR-expressing plasmid pGS058 was then introduced to confirm that the *ahpC′-lacZ* fusion was OxyR responsive. An approximately 40-fold increase in activity was observed.

The responsiveness of the *degP-lacZ* fusion to standard DegP inducing conditions (37) was tested by culturing cells to an OD_{600} of 0.2 in LB medium containing 0.5% SDS and 0.5 mM EDTA at 42°C, in parallel with a culture in plain LB medium at 37°C. A 3-fold induction of β-galactosidase activity was observed.

All of the other mutations were moved into the strains by P1 transduction (33). Transduction of the Δ*ahpCF* mutation into the Δ*katE* Δ*katG* mutant background, of the Δ*oxyR* mutation into the wild-type background, and of all mutations into the hydroperoxidase-deficient (Hpx$^-$) and Δ*oxyR* mutant backgrounds was performed by infecting cells aerobically and then selecting transductants on anaerobic plates in the Coy chamber. Because trace amounts of H_2O_2 contaminate laboratory media, it was necessary to add catalase to plating medium in order to obtain Δ*oxyR* transductants. For this purpose, catalase (stock concentration, 30,000 U/ml) was diluted 1:10 into the transduction mix immediately prior to spreading.

The chloramphenicol-sensitive versions of SRK9, SRK27, and SRK35 strains were constructed by removing the chloramphenicol cassette fused with *ahpCF* using temperature-sensitive, ampicillin-resistant pCP20 that encodes FLP recombinase. The mutant strains were then made to lose pCP20; hence, they became ampicillin sensitive.

Δ*tynA*, Δ*rpoS*, Δ*sufABCDSE*, Δ*dps*, Δ*recA*, Δ*oxyR*, Δ*mntH*, Δ*ahpCF*, and Δ*katE* transductants were confirmed by colony PCR (PuRe *Taq* ready-to-go PCR beads; GE Healthcare). Δ*katG* and Δ*katE* Δ*katG* mutants were screened by adding a drop of 30% H_2O_2 to colonies that had been restreaked on LB medium and grown overnight; Δ*katG* mutants form noticeably smaller bubbles than do wild-type cells, and Δ*katE* Δ*katG* mutants form no bubbles at all. The *polA1* transductants were confirmed by UV sensitivity.

Standard growth studies. To obtain information about growth rates, strains from defined medium plates were cultured overnight in liquid of the same composition. The overnight cultures were then diluted to an OD_{600} of 0.005 in fresh medium and grown to an OD_{600} of 0.1. These precultured cells were then inoculated into 15 ml of fresh medium to an OD_{600} of 0.015; the OD_{600} of the culture was subsequently monitored. In some cases (when indicated), the medium used in preculture and final culture differed. When cells were shifted to a medium of different composition, they were first washed using 0.1 M KH_2PO_4 (pH 7.1) buffer.

Phenylethylamine utilization rate experiment. The rate of phenylethylamine utilization was determined by measuring the maximum biomass achieved in cultures containing a range of PEA concentrations when PEA was used either as the sole carbon or sole nitrogen source. These data provided the value for mM PEA consumed per OD unit of biomass. This value was multiplied by the growth rate constant, which was determined from the growth equation $\mathrm{Ln}(OD/OD_i) = kt$, where k is the rate constant and t is the time interval between the initial (i) and final optical density measurements. The result is the PEA consumption rate from the medium, expressed as the millimolar concentration per OD unit per hour. Since 1 ml of biomass at an OD_{600} of 1 comprises a 0.47-μl cell volume (38), the rate of PEA consumption from the medium was converted to the rate of PEA consumption inside the cells by multiplying by 2,130 (ml culture/ml cells). Since 1 molecule of H_2O_2 is produced per molecule of PEA consumed, this rate also represents the rate of intracellular H_2O_2 formation. The periplasm constitutes about 20% of the cell volume (39), so the specific rate of periplasmic H_2O_2 formation was obtained by multiplying the total cell rate by five.

Our data (see Results) indicated that 2.8 mM PEA was required per OD unit of final biomass. This value was compared to the reported nitrogen content of *E. coli*. We typically obtained ~190 mg total protein per liter per OD unit of cells. Using the values that the protein represents 55% of dry weight and the dry weight is 14% nitrogen (40), we calculate that 1 liter of cells at an OD of 1 should contain 3.4 mmol of nitrogen. These numbers predict that 3.4 mM PEA should be required to generate cells at an OD of 1, which, given the approximations involved, is in good agreement with our measured value of 2.8 mM PEA.

Enzyme assays. Enzyme activities were typically measured for exponentially growing cells after a period of preculture and subsequent dilution and growth to an OD_{600} of 0.1 to 0.2. Thus, exponential-phase en-

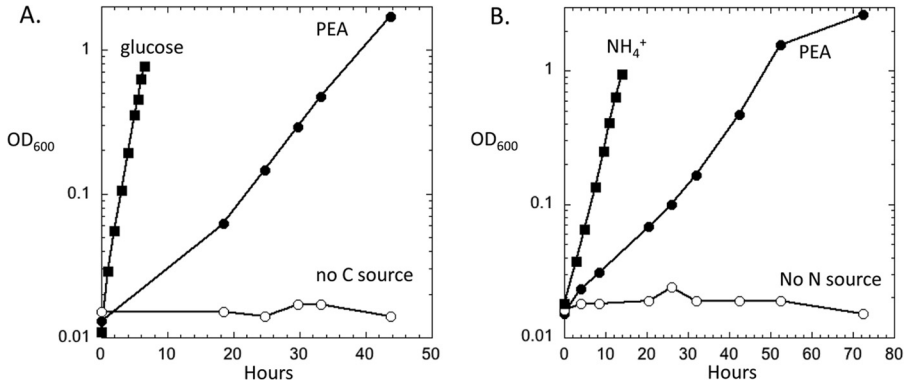

FIG 2 *E. coli* can use phenylethylamine as a sole carbon or nitrogen source. (A) The wild-type strain W3110 was grown in medium containing PEA as the carbon source and ammonium as the nitrogen source. At time zero, the cells were washed and inoculated into medium containing 0.2% glucose, 10 mM PEA, or no carbon source. The doubling time in PEA medium was 5 to 6 h. (B) A growing culture of W3110 in medium containing glycerol as the carbon source and PEA as the nitrogen source was washed and inoculated into glycerol medium containing 10 mM ammonium, PEA, or no nitrogen source. The doubling time in PEA-containing medium was 4.5 to 5.5 h.

zyme activities represent values for cells that had undergone at least five doublings in the relevant growth medium. At the indicated time points, cells were centrifuged at 4,000 rpm for 10 min at 4°C. The cell pellet was washed twice with appropriate buffers. The cells were lysed using a French press, and the samples were centrifuged at 12,000 rpm for 20 min at 4°C. The supernatant obtained was used for assays.

Monoamine oxidase activity was assayed by tracking the formation of the carbonyl group of its phenylacetaldehyde product. This is a discontinuous colorimetric assay (20). A 4-ml reaction mixture was constituted by the consecutive addition of potassium phosphate buffer, pH 6.1 (87.5 mM final concentration); crude extract; and 2-phenylethylamine · HCl (5 mM final concentration). At timed intervals over 15 min, a 1-ml sample from the mixture described above was added to 0.33 ml of 0.1% 2,4-dinitrophenylhydrazine · HCl in 2 M HCl. This was incubated at room temperature in the dark for 10 min, and then 1.67 ml of 10% NaOH was added. After incubation for 60 min at room temperature in the dark, the absorbance was measured at A_{435}. One μM PAA equates to 2.5 absorbance units.

β-Galactosidase activity was measured in cell extracts by a standard assay with *o*-nitrophenyl-β-D-galactopyranoside (33). Cultures (20 to 40 ml) were washed and suspended in 2 ml prior to lysis. The activity of β-galactosidase was calculated (1 U = 1 μmol product/min) using 4,500 M^{-1} cm^{-1} as the extinction coefficient for *o*-nitrophenol.

Catalase activity was measured using 50-ml cultures at an OD_{600} of 0.1 to 0.2. After preparation of the extract, 10 mM H_2O_2 was added and the decrease in H_2O_2 concentration was monitored by absorbance at 240 nm (41).

Total protein concentrations of cell extracts were determined using the Thermo Scientific Pierce Coomassie plus (Bradford) protein assay, with BSA as a protein standard.

Modeling of cytoplasmic, periplasmic, and extracellular H_2O_2 concentrations. The flux equations that were used to generate Fig. 11 are presented, explained, and worked out in the supplemental material. Calculations were performed for steady-state situations. This is valid because the steady-state situation is almost immediately achieved for the scenarios depicted in Fig. 11A and B. It is shown in the calculations that the steady-state H_2O_2 concentrations depicted in Fig. 11C would be achieved on a 10-min time scale at the cell densities used in this paper; thus, the results pertain to the experiments reported in it. At the lower cell densities that might be found in nature, e.g., 10^5 cells/ml rather than 10^7 cells/ml, it would require far longer for environmental H_2O_2 to accumulate, and Fig. 11B would be a better representation of the outcome.

RESULTS

***E. coli* can utilize phenylethylamine as sole carbon or nitrogen source.** The *E. coli* K-12 wild-type strain W3110 was able to grow on plates that contained phenylethylamine (PEA) as either a sole carbon or sole nitrogen source. The pathway of PEA catabolism is denoted in Fig. 1. As expected, deletion of the *tynA* gene, which encodes Cu-MAO, prevented growth on PEA, while the *tynA* mutant was able to grow when phenylacetic acid (PAA) was provided. PEA-dependent growth was only possible in aerobic medium, consistent with the fact that Cu-MAO requires oxygen as a coreactant.

We sought growth conditions that maximized the flux through Cu-MAO. Growth in liquid medium was established using M63 salts base. Growth behavior was more consistent at 30 than 37°C, as others have noted (20), so the majority of experiments were conducted at the lower temperature. To improve the growth rate, we routinely supplemented the media with six amino acids that *E. coli* cannot catabolize (Lys, Val, Ile, Leu, His, and Met). Doubling times of 5 to 6 h were typically observed when PEA was the sole carbon source (Fig. 2A). When PEA was supplied as the sole nitrogen source in amino-acid-free glycerol medium, growth was slightly faster (ca. 5-h doubling times) (Fig. 2B).

The Cu-MAO activity was high when cells were cultured in PEA medium (0.050 ± 0.009 U/mg) but below detection in PAA medium (<0.004 U/mg). Supplementation of the medium with extra copper to metallate Cu-MAO neither accelerated the growth rate nor increased the Cu-MAO activity. Evidently the trace copper that contaminates M63 base medium was sufficient to fully activate the enzyme. Media without extra copper were used in the experiments described below (as indicated).

We wished to determine the rate at which Cu-MAO generates H_2O_2 during PEA catabolism. To do so, we quantified the rate of PEA degradation, which occurs in a 1:1 stoichiometry with H_2O_2 formation. Limiting concentrations of PEA were supplied, enabling us to quantify the relationship between the amount of PEA degraded and the amount of biomass produced. Figure 3 depicts the final yields when various concentrations of PEA were employed as carbon (Fig. 3A) or nitrogen (Fig. 3B) sources. When used as a carbon source, 5.0 mM PEA was required per unit of

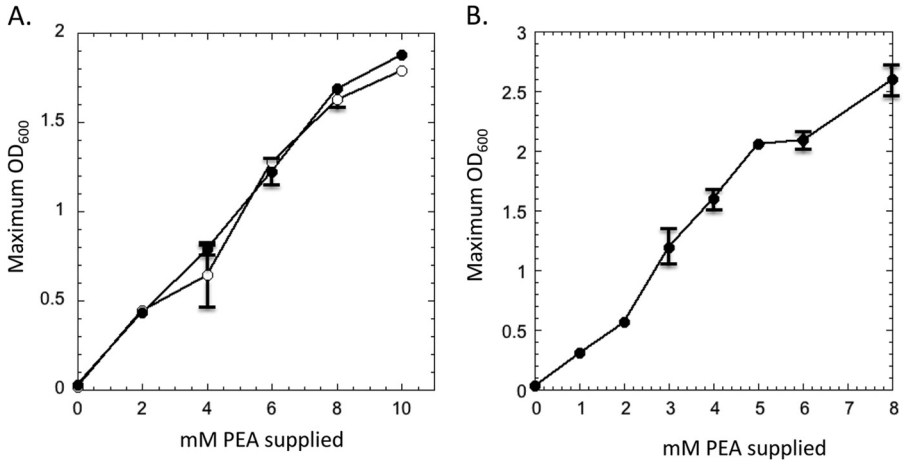

FIG 3 Dependence of biomass upon the supplied concentration of PEA. Data points indicated the final optical density achieved. (A) PEA was supplied as the sole carbon source (with ammonium as the nitrogen source). The base medium was supplemented with 1 μM copper sulfate (open symbols). (B) PEA was supplied as the sole nitrogen source (with glycerol as the carbon source). Error bars represent the standard deviations from three independent samples.

biomass at an OD_{600} of 1.0. As expected, less PEA was needed to support equivalent growth when it served as a nitrogen source: 2.8 mM per OD unit. This value is a good fit to the reported nitrogen content of *E. coli* (see Materials and Methods). Growth rates were 0.126 h^{-1} (PEA as carbon source) and 0.139 h^{-1} (PEA as nitrogen source). Therefore, the consumption of PEA from the medium in which it served as a carbon source was as follows: 0.126 h^{-1} × 5 mM/OD unit = 0.63 mM/h/OD unit. Our prior measurements have shown that 1.0 OD unit of *E. coli* in defined medium comprises 4.7×10^{-4} of the culture volume (38), so that one can deduce that PEA consumption occurred at a rate of 370 μM/s when normalized to the total intracellular volume (cytoplasm plus periplasm) (Table 1). Similar calculations for cells using PEA as a nitrogen source produce a rate of 230 μM/s.

Therefore, these values also represent the rates of intracellular H_2O_2 formation. Direct measurements have shown that cells grown on a range of other carbon sources, such as glucose, succinate, glycerol, etc., produce about 12 μM/s H_2O_2 (1). Thus, PEA catabolism generates H_2O_2 at a rate that is 30-fold higher than is usual. The difference is 20-fold when PEA is utilized only as a nitrogen source.

Use of phenylethylamine turns on the cellular stress regulon to act against hydrogen peroxide. Excessive cytoplasmic H_2O_2 oxidizes a critical cysteine residue of OxyR, triggering the formation of a disulfide bond that locks OxyR into a conformation that activates it as a transcription factor (42). Steady-state intracellular H_2O_2 concentrations of 0.1 to 0.2 μM are thought to be sufficient (43, 44). During growth in standard media, H_2O_2 levels are believed to be ~50 nM (13); thus, OxyR is not activated in standard glucose or glycerol media. To date, OxyR has been observed to be activated only when high levels of environmental H_2O_2 flow into the cell. As little as 5 μM exogenous H_2O_2 has been observed to activate intracellular OxyR (43).

We wondered whether OxyR was activated by the H_2O_2 released by the Cu-MAO enzyme activity. Catalase, encoded by *katG*, is one of the enzymes that are induced in response to OxyR. Indeed, total catalase activity was elevated when cells were grown using PEA as a carbon source but not when PAA was supplied instead (Fig. 4A). Parrott et al. also noted an increase in catalase activity during PEA catabolism (20). Since *E. coli* also has a second catalase, encoded by *katE*, that is induced by the RpoS response to nutritional limitations, a *katG*::*lacZ* transcriptional fusion was used to specifically monitor *katG* promoter activity by measurement of β-galactosidase activity. The *katG* promoter activity showed 2- to 3-fold higher expression in PEA medium than in PAA medium. This effect was absent from Δ*oxyR* mutants. The *ahpCF* operon is also controlled by OxyR, and an *ahpC*::*lacZ* fusion was similarly induced in PEA medium (Fig. 5A).

NADH peroxidase (Ahp) is the primary scavenger of endogenous H_2O_2 during growth in glucose media, so Δ*ahp* mutants exhibit some induction of the OxyR regulon on all tested media (44). Indeed, the *katG*::*lacZ* fusion was partially induced in Δ*ahp* mutants grown in PAA medium. It was much more strongly induced in PEA medium, matching the pattern observed in scavenger-proficient cells (Fig. 5B). This result confirms that higher *katG* expression was driven by H_2O_2 levels, and it indicates that in PEA medium Ahp remained the primary scavenger of H_2O_2.

Close inspection revealed that when cells were shifted from PAA medium to PEA medium, their growth lagged for about 15 h (Fig. 6). This stasis presumably correlates to the time required to synthesize and activate Cu-MAO. The induction of *katG* occurred upon the resumption of growth, consistent with the point at which H_2O_2 production would begin.

OxyR induction is necessary for utilization of phenylethylamine as a carbon source. The Δ*oxyR* mutant grew poorly on PEA plates (not shown). To test this phenotype in liquid media, cells that were growing exponentially in PAA medium were washed and inoculated into PEA medium. Again we observed that after a

TABLE 1 Rates of PEA utilization by W3110

Growth medium	Doubling time (h)	PEA concn (mM) to achieve OD_{600} of 1.0	H_2O_2 formation (μM/s) in cell
PEA as C source, NH_4^+ as N source	5.5 ± 0.5	5.0	370 ± 50
Glycerol as C source, PEA as N source	5.0 ± 1.0	2.8	230 ± 40

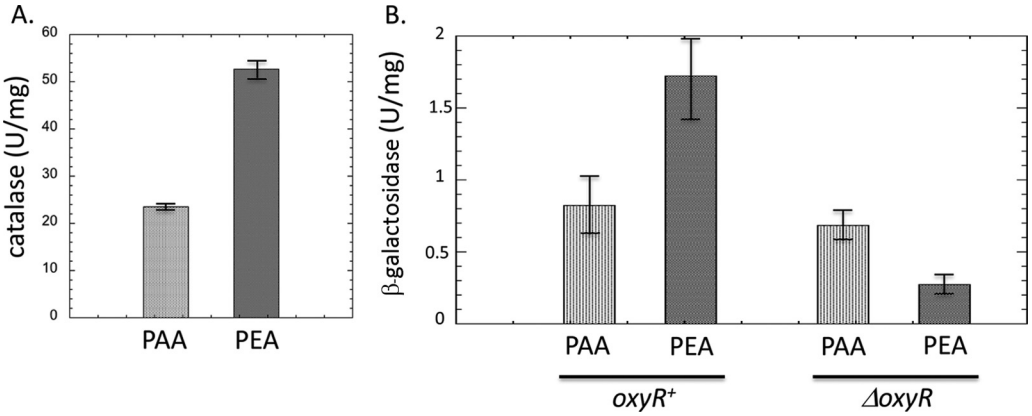

FIG 4 Catalase is induced during growth in PEA medium. (A) Total catalase activity was measured in exponentially growing cells in PEA and PAA media. Error bars represent standard deviations from three independent samples. (B) β-Galactosidase activity from a *katG*::*lacZ* fusion was measured in exponentially growing cultures of OxyR$^+$ (SRK5) and OxyR$^-$ (SRK14) cells in PEA and PAA media. Note that the OxyR$^-$ strain grew poorly in PEA medium.

lag period of about 10 h, the wild-type cells started to grow; they continued to do so to an OD_{600} of >1 (Fig. 7A). In contrast, the Δ*oxyR* mutant started to grow, but it did so at lower rates than the wild-type cells, and the growth slowed and finally stopped after about 25 to 30 h. The cells remained static for another 20 to 30 h, and eventually their OD_{600} values began to drop. The *oxyR* mutation did not disrupt growth in PAA medium (Fig. 7B), confirming that the role of the OxyR regulon in PEA medium is to defend the cell against H_2O_2 generated by Cu-MAO.

Hydrogen peroxide scavengers that are regulated by OxyR are essential for growth on PEA. *E. coli* hydroperoxidase (Hpx$^-$) mutants (11) lack its three scavenging enzymes, catalase E, catalase G, and NADH peroxidase (Ahp), and cannot grow in glucose medium unless aromatic amino acids are provided. This defect reflects the inactivation of a shikimate pathway enzyme by endogenous H_2O_2 (unpublished data). To test the viability of Hpx$^-$ mutants (Δ*katE* Δ*katG* Δ*ahpCF*) in solid PAA and PEA media, colonies pregrown in anaerobic glycerol/nitrate medium were restreaked on aerobic PAA and PEA media that were supplemented with Phe, Trp, and Tyr. Cells grew on PAA plates but not on PEA plates, even after 7 days of incubation. This observation was reproduced in liquid media (Fig. 8A and B). Transfer from PAA to PEA medium also led to permanent stasis of the Hpx$^-$ mutant (Fig. 8C). These results confirm prior workers' suspicions that PEA catabolism is not possible in strains that lack H_2O_2 scavengers (20).

We then wanted to move forward and see which of the H_2O_2 scavenging enzymes is critical for the cells to survive in PEA medium. Exponentially growing Ahp$^-$ cells in PAA medium were washed and inoculated into PEA and PAA media (Fig. 9). The strain grew slightly more poorly in PAA medium than did the wild-type or catalase-deficient strains, which matches the slight growth defect that is also seen in glucose medium (not shown). However, the growth defect in PEA medium was much more severe, with growth progressively slowing to a doubling time of 40 h. Evidently the induction of catalase (Fig. 5B) does not fully compensate for the absence of Ahp. In contrast, a strain lacking both catalases grew as well as the wild type.

Other OxyR-induced proteins include Dps, an iron-sequestering protein that suppresses Fenton chemistry (5, 29, 45, 46); MntH, a manganese importer that enables the replacement of iron by manganese in mononuclear enzymes (30, 47); and the Suf machinery, which enables the continued synthesis of iron-sulfur clusters when high concentrations of H_2O_2 disrupt function of the housekeeping Isc system (32, 48). None of these proteins was necessary for growth in PEA medium (see Fig. S1 to S3 in the supplemental material). The Δ*mntH* strain consistently exhibited a slightly longer lag, but the effect was minor and transient. Moreover, although RecA protein and DNA polymerase I are each critical for the repair of oxidative DNA lesions (49), mutations in *recA* and *polA* had little impact upon growth in PEA (see Fig. S4). We infer that when Ahp is functional and inducible, the level of cyto-

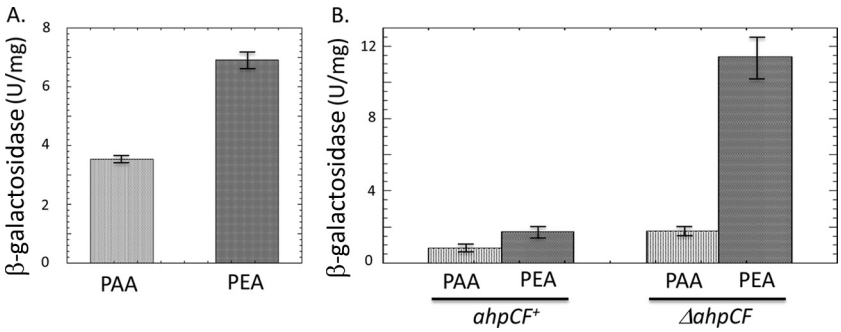

FIG 5 *ahpCF* genes are involved in growth on PEA medium. (A) An *ahpC*::*lacZ* fusion was induced in PEA medium. Strain SRK57 was used. (B) A *katG*::*lacZ* fusion was more strongly induced in PEA medium in a strain lacking Ahp. The strains were SRK5 (Ahp$^+$) and SRK17 (Ahp$^-$).

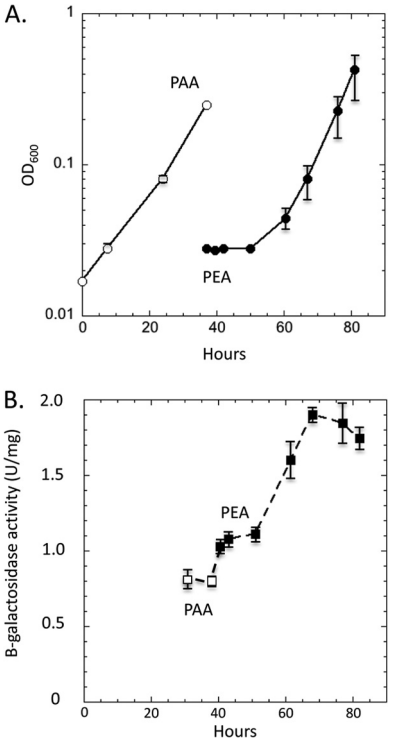

FIG 6 *katG*::*lacZ* induction occurs during the period of outgrowth in PEA medium. Strain SRK5 (*katG*::*lacZ*) was precultured in PAA medium and subcultured at time zero into fresh PAA medium. At 36 h the strain was washed and suspended in fresh PEA medium. Optical density was tracked (A), and at intervals samples were harvested and β-galactosidase was measured (B). Open symbols represent measurements in PAA medium, and closed symbols represent measurements in PEA medium.

plasmic H_2O_2 does not rise high enough to create disabling levels of damage to mononuclear enzymes, the Isc system, or DNA.

Activation of other stress regulons during PEA catabolism. Finally, we also tested whether RpoS assists growth in PEA, since this sigma factor activates protective systems, including oxidative defenses, when *E. coli* struggles to grow (50). However, an *rpoS* deletion had no significant impact upon the growth phenotype (see Fig. S5 in the supplemental material), indicating that this general response to cytoplasmic stress was not critical.

Cu-MAO is located in the periplasm, and one would expect H_2O_2 levels to be higher in this compartment than in the cytoplasm itself. The Cpx system responds to stresses that perturb the envelope environment (51). A *degP*::*lacZ* fusion was generated, since *degP* is an established member of the Cpx regulon. It responded as expected to known inducing conditions (42°C in SDS). Strikingly, it was also induced during growth on PEA but not PAA (Fig. 10A).

The DsbG protein is a reductase of periplasmic proteins containing sulfenic acids (52). It is expressed as part of the OxyR response, and we thought it might help protect periplasmic proteins from Cu-MAO-generated H_2O_2. However, mutants did not display any growth defect under the conditions that were used (Fig. 10B).

DISCUSSION

The oxidative deamination of primary amines by MAOs requires their oxidation to an imine intermediate (53). Like most desaturation reactions, this requires a sufficiently strong electron acceptor, and NAD^+ (−0.32 V) is not a feasible coreactant. For this reason, the electrons are transferred directly to either enzymatic flavins (~−0.22 V) or topoquinones (+0.079 V) that have higher intrinsic potentials. The enzyme cofactor is subsequently recycled via electron transfer to molecular oxygen, whose divalent reduction potential is even more positive (+0.39 V for 1 M O_2). The favorable thermodynamics allow aliphatic amines to be efficiently oxidized, but the H_2O_2 by-product is a potential hazard for the cell.

How effectively does the cytoplasmic membrane shield the cytoplasm from H_2O_2 that is formed in the periplasm? In mammalian cells, MAOs oxidize histamines, drugs, and neurotransmitters, and since these fluxes are likely to be low, the enzymes may not contribute much stress against the background of chronic H_2O_2 formation by adventitious oxidation of redox enzymes. In contrast, Cu-MAO poses a dilemma for bacteria because it is a high-flux enzyme. Our calculations (see the supplemental material) reveal that its rate of H_2O_2 formation is high enough that if it occurred in the cytoplasm, H_2O_2 levels would immediately rise to micromolar levels (Fig. 11A). These concentrations are sufficient to poison vulnerable enzymes and thereby paralyze key metabolic pathways, including those for aromatic and branched-chain syn-

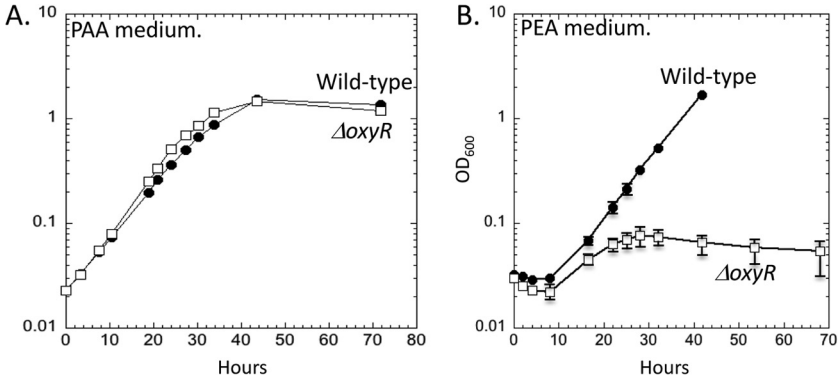

FIG 7 Induction of the OxyR regulon is essential for growth in PEA medium. Exponentially growing wild-type (W3110) and OxyR$^-$ (SRK11) cultures in PAA medium were washed and diluted into PAA (left) or PEA (right) medium. Error bars represent the standard deviations from three independent cultures. Where error bars are not visible, they are obscured by the data symbol.

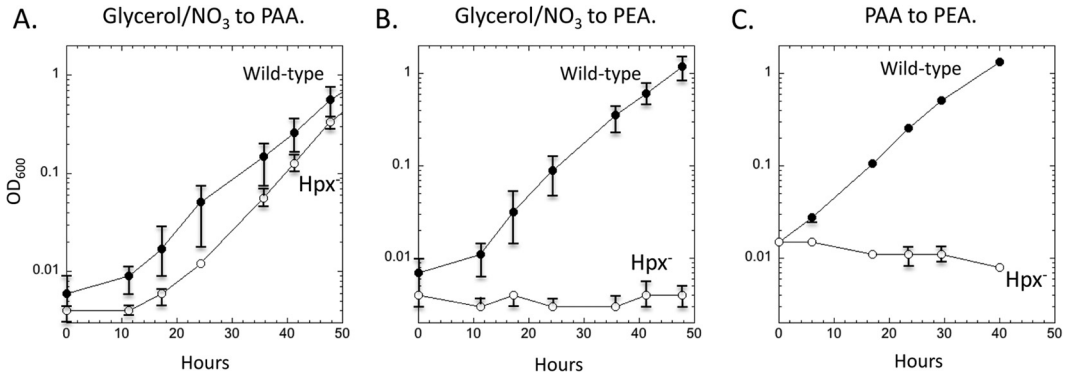

FIG 8 Mutants that lack H_2O_2 scavenging enzymes (Hpx^-) cannot grow in PEA medium. (A and B) Exponentially growing cultures in anaerobic glycerol/nitrate medium were washed and inoculated at time zero into PAA (A) or PEA (B) media. (C) Cells growing exponentially in aerobic PAA medium were washed and inoculated at time zero into PEA medium. Wild-type cells were W3110. Hpx^- mutants (SRK27; Δ*ahpCF* Δ*katG* Δ*katE*) cannot efficiently scavenge H_2O_2 due to absence of NADH peroxidase (Ahp) and both catalase isozymes.

thesis, the tricarboxylic acid (TCA) cycle, and the pentose-phosphate pathway (2–4).

E. coli circumvents this hazard in two ways. Most notably, it localizes Cu-MAO in the periplasm. This is not a common site for catabolic enzymes: only a half dozen enzymes that operate on typical small-molecule substrates are located there (http://db.psort.org/). Indeed, the remaining enzymes of the PEA catabolic pathway are cytoplasmic. This circumstance suggests that by generating the H_2O_2 outside the cytoplasm, the cell minimize oxidative damage to cytoplasmic enzymes and nucleic acids.

At first blush, an alternative reason for periplasmic localization can be proposed. Cu-MAO is a copper-requiring enzyme, and it appears that in general *E. coli* avoids the toxic effects of this soft metal by exiling it to the periplasm (54). For this reason, the other copper-dependent enzymes of the cell are either localized here (the multicopper oxidase and copper/zinc superoxide dismutase) or loaded with copper from here (the cytochrome *bo* oxidase). However, flavin-dependent MAOs are common in nature (55), so a simpler arrangement would be for *E. coli* to rely upon a cytoplasmic flavin MAO. Because flavins are not exported to the periplasm, it is more likely that the periplasmic localization of the *E. coli* MAO is the basis for its utilization of topaquinone and copper rather than vice versa.

How effectively does this compartmentalization shield cytoplasmic enzymes from the H_2O_2 that Cu-MAO makes? The key determinant is whether H_2O_2 will diffuse passively through the porins of the outer membrane and out of the cell more rapidly than it will traverse the lipid bilayer of the inner membrane and enter the cytoplasm. This intuitive expectation can be tested by comparing the permeability coefficients of the cytoplasmic and outer membranes to H_2O_2. Although H_2O_2 has sometimes been casually described as freely crossing membranes, this is a significant misrepresentation, as membranes retard H_2O_2 flow sufficiently well that transmembrane concentration differences can arise. In prior work, we measured the coefficient of the *E. coli* inner membrane for H_2O_2 to be 1.6×10^{-3} cm/s (44), and this value was subsequently confirmed (56). That of the outer membrane has not been determined for H_2O_2 itself, but it has been measured to be about 4×10^{-3} cm/s for glucose and 10-fold higher (ca. 50×10^{-3} cm/s) for glycerol (57). This difference arises from the smaller hydration radius of glycerol compared to that for glucose; thus, the coefficient of H_2O_2 is certain to be higher still. Therefore, the permeability of the outer membrane to H_2O_2 is >30-fold higher than that of the inner membrane. It follows that virtually all H_2O_2

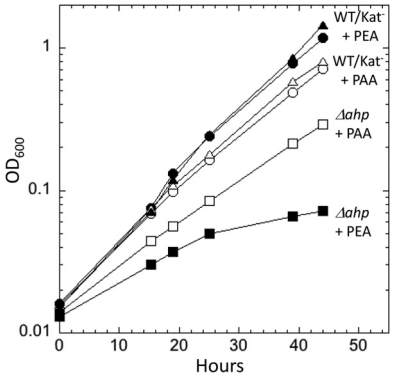

FIG 9 Ahp is critical for growth in PEA medium, but catalase is not. Cells growing exponentially in PAA medium were washed and inoculated at time zero into either PAA medium (open symbols) or PEA medium (closed symbols). The strains were W3110 (wild type; circles), SRK29 (Kat^-; triangles), and SRK9 (Δ*ahp*; squares).

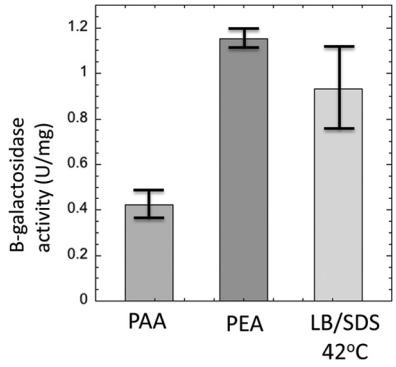

FIG 10 PEA catabolism activates the periplasmic stress response. (A) A *degP*::*lacZ* fusion strain (SRK65) was grown to exponential phase in 30°C PAA medium, 30°C PEA medium, or 42°C LB medium containing SDS-EDTA.

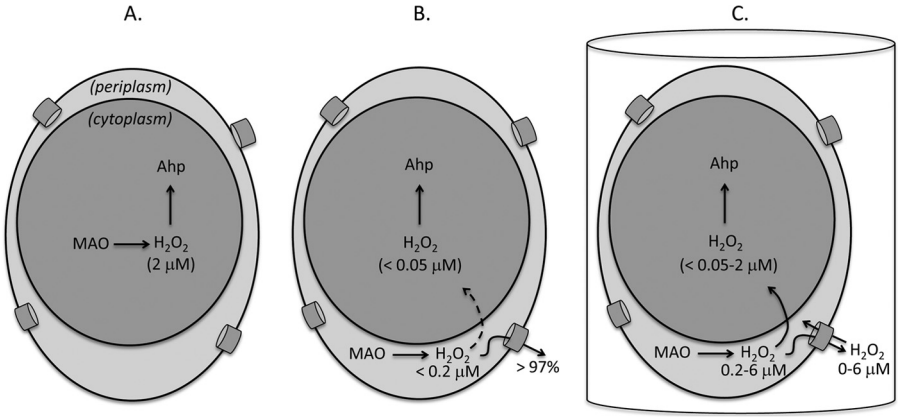

FIG 11 Periplasmic localization of phenylethylamine oxidase should shield the cytoplasm from H_2O_2 stress. Calculations are based on the basal titers of Ahp and catalase. See Materials and Methods for details. (A) If the oxidase were located in the cytoplasm, H_2O_2 levels would rapidly rise to 1 to 2 μM. (B) The oxidase is actually located in the periplasm. Calculations show that virtually all H_2O_2 would efflux out of the cell and be lost to an open environment. (C) In laboratory experiments the H_2O_2 that is released by cells gradually accumulates in the local environment and will approach a limit of ~6 μM. The time that this requires will depend upon cell density. Equilibration across the outer membrane will drive periplasmic H_2O_2 to an equivalent concentration, and influx across the cytoplasmic membrane will ultimately raise cytoplasmic levels to 1 to 2 μM. Induction of scavenging enzymes will then diminish this concentration.

that is generated in the periplasm will flow out of the cell rather than into the cytoplasm (Fig. 11B). In the natural oxic habitats of aerobic *E. coli* (ponds, for example), the excreted H_2O_2 would be lost to the environment. The amount of H_2O_2 that instead penetrates the cytoplasmic membrane (<10 μM/s) would be smaller than the amount already being made there by adventitious enzyme autoxidation processes. Thus, the localization of MAO in the periplasm is a very effective way of shielding cytoplasmic enzymes from the H_2O_2 that it generates.

Analogous roles for the periplasm, peroxisomes, and bacterial microcompartments. Interestingly, higher eukaryotes face a similar threat from H_2O_2-generating oxidases. Almost 250 such enzymes are documented in MetaCyc (www.metacyc.org/). Many of these are probably made in small amounts, and others may be misunderstood. Some oxidases involved in heme synthesis, for example, may actually use respiratory quinones rather than oxygen as their direct electron acceptor; the oxidase activity that is detectable *in vitro* may be artifactual autoxidation that slowly occurs when the physiological acceptor is not provided. (Notably, the *E. coli* "protoporphyrinogen oxidase" continues to function *in vivo* in anaerobic habitats [58].) However, a number of high-flux oxidases are also found, including those required for the β-oxidation of very-long-chain fatty acids, the purine salvage pathway, oxidative deamination of D-amino acids, and glycolate oxidation (59). These enzymes are colocalized along with high titers of catalases and peroxidases in peroxisomes, a relatively impermeable compartment whose role is to shield the cell from major sources of H_2O_2. In this regard the eukaryotic peroxisome and the bacterial periplasm appear to serve the same purpose.

Interestingly, bacteria must cope with an analogous situation when pathways involve the production of reactive aldehydes as intermediates. The distinction is that the efflux of H_2O_2 from the cell is to its benefit, whereas aldehydes must be contained for further catabolism. In several cases toxicity is averted through the encapsulation of the aldehyde-producing and consuming reactions in bacterial microcompartments (BMCs), which are essentially protein-bounded organelles that are analogues of eukaryotic peroxisomes (60). Well-studied examples include BMCs that drive propanediol, ethanolamine, and ethanol catabolism. This arrangement is expensive for the cell, however, because it entails the assembly of a large protein shell, as well as the proteins that presumably enable metabolite entry and egress. In comparison, the secretion of Cu-MAO to the periplasm is a simpler, more economical solution.

When *E. coli* generates extracellular H_2O_2 in a closed environment, the OxyR system is a key defense. The current study involved pure cultures of *E. coli*, and as a result, the H_2O_2 that was released by the cells remained in its immediate environment rather than being swallowed by the external world. Whether *E. coli* enters such enclosed microhabitats in nature is uncertain. In a closed system the accumulation of extracellular H_2O_2 ensures that it ultimately flows back into the cell, gradually raising cytoplasmic H_2O_2 concentrations (Fig. 11C). Because of this circumstance, the OxyR regulon was needed to ward off damage. The Ahp peroxidase and KatG catalase were the primary defenses; evidently the H_2O_2 dose was not high enough to require the function of other members of the regulon. Nevertheless, this comprises the first example in which the OxyR response was needed to cope with a natural, endogenous source of H_2O_2. It is, of course, possible that other such situations are found in bacteria and that alleviation of endogenous stress is a significant function of OxyR in some microbes.

We anticipated that DsbG, which has been proposed to reverse the oxidation of cysteine residues on periplasmic proteins (52), is important in this situation, but this was not the case. Adjusting for the fact that the periplasm is only about 20% of the cell volume and that Cu-MAO produces a flux of H_2O_2 that is 30-fold greater than the cumulative 10 μM/s generated by cytoplasmic sources, it follows that Cu-MAO generates H_2O_2 within the periplasm at a rate of about 1.5 mM/s. However, efflux through the outer membrane should be fast enough that the steady-state concentration rises no higher than 0.2 μM. If H_2O_2 accumulates in the environment and reenters the cell, the maximum H_2O_2 level might rise as high as 6 μM. The rate constant for the oxidation of typical cysteine residues (ca. 10 M^{-1} s^{-1} [61]) implies that at this concentration, the half-time for thiol oxidation would be about 4 h. PEA

catabolism activated synthesis of periplasmic DegP, suggesting that the Cpx system responded to periplasmic protein damage. It is not apparent whether the source of stress was the H_2O_2 or the aldehydes that Cu-MAO makes.

Finally, we note that Cu-MAO activity was evidently lost in many *E. coli* laboratory isolates. This study employed a W3110 isolate obtained from one laboratory. In contrast, W3110, obtained from a second laboratory, grew robustly on PAA, but it formed only a few tiny colonies on PEA solid medium and none in liquid medium. However, cultivation of the few colonies allowed the quick isolation of good growers. Other *E. coli* K-12 strains varied in their behavior: MG1655 and AN387 stocks could utilize PEA on plates as either a carbon or nitrogen source, while CSH7 could not. The basis of the defects is not clear, although we speculate that due to the H_2O_2 stress that it can impose, Cu-MAO may have been selected against during the decades in which these strains were maintained in room-temperature stabs. Interestingly, MAO activity is also easily lost when mammalian cells are maintained in culture (62).

These results may be of practical interest to metabolic engineers who wish to direct high substrate fluxes through H_2O_2-producing pathways. Cytochrome P450 enzymes have been the frequent subjects of such efforts, and these enzymes produce significant H_2O_2 through uncoupled catalytic cycles (63). The implication is that the H_2O_2 these enzymes release in the cytoplasm debilitate the cell. A first test of that notion would include measurements of whether the OxyR response is activated.

ACKNOWLEDGMENTS

We thank Sergei Korshunov for helpful conversations and experimental assistance.

This work was supported by GM049640 from the National Institutes of Health.

REFERENCES

1. **Seaver LC, Imlay JA.** 2004. Are respiratory enzymes the primary sources of intracellular hydrogen peroxide? J. Biol. Chem. **279:**48742–48750.
2. **Jang S, Imlay JA.** 2007. Micromolar intracellular hydrogen peroxide disrupts metabolism by damaging iron-sulfur enzymes. J. Biol. Chem. **282:**929–937.
3. **Sobota JM, Imlay JA.** 2011. Iron enzyme ribulose-5-phosphate 3-epimerase in *Escherichia coli* is rapidly damaged by hydrogen peroxide but can be protected by manganese. Proc. Natl. Acad. Sci. U. S. A. **108:**5402–5407.
4. **Anjem A, Imlay JA.** 2012. Mononuclear iron enzymes are primary targets of hydrogen peroxide stress. J. Biol. Chem. **287:**15544–15556.
5. **Park S, You X, Imlay JA.** 2005. Substantial DNA damage from submicromolar intracellular hydrogen peroxide detected in Hpx$^-$ mutants of *Escherichia coli*. Proc. Natl. Acad. Sci. U. S. A. **102:**9317–9322.
6. **Massey V, Strickland S, Mayhew SG, Howell LG, Engel PC, Matthews RG, Schuman M, Sullivan PA.** 1969. The production of superoxide anion radicals in the reaction of reduced flavins and flavoproteins with molecular oxygen. Biochem. Biophys. Res. Commun. **36:**891–897.
7. **Grinblat L, Sreider CM, Stoppani AO.** 1991. Superoxide anion production by lipoamide dehydrogenase redox-cycling: effect of enzyme modifiers. Biochem. Int. **23:**83–92.
8. **Messner KR, Imlay JA.** 1999. The identification of primary sites of superoxide and hydrogen peroxide formation in the aerobic respiratory chain and sulfite reductase complex of *Escherichia coli*. J. Biol. Chem. **274:**10119–10128.
9. **Messner KR, Imlay JA.** 2002. Mechanism of superoxide and hydrogen peroxide formation by fumarate reductase, succinate dehydrogenase, and aspartate oxidase. J. Biol. Chem. **277:**42563–42571.
10. **Korshunov S, Imlay JA.** 2010. Two sources of endogenous hydrogen peroxide in *Escherichia coli*. Mol. Microbiol. **75:**1389–1401.
11. **Seaver LC, Imlay JA.** 2001. Alkyl hydroperoxide reductase is the primary scavenger of endogenous hydrogen peroxide in *Escherichia coli*. J. Bacteriol. **183:**7173–7181.
12. **Link AJ, Robison K, Church GM.** 1997. Comparing the predicted and observed properties of proteins encoded in the genome of *Escherichia coli* K-12. Electrophoresis **18:**1259–1313.
13. **Imlay JA.** 2013. The molecular mechanisms and physiological consequences of oxidative stress: lessons from a model bacterium. Nat. Rev. Microbiol. **11:**443–454.
14. **Rankin LD, Bodenmiller DM, Partridge JD, Nishino SF, Spain JC, Spiro S.** 2008. *Escherichia coli* NsrR regulates a pathway for the oxidation of 3-nitrotyramine to 4-hydroxy-3-nitrophenylacetate. J. Bacteriol. **190:**6170–6177.
15. **Hamana K, Niitsu M.** 1999. Production of 2-phenylethylamine by decarboxylation of L-phenylalanine in alkaliphilic *Bacillus cohnii*. J. Gen. Appl. Microbiol. **45:**149–153.
16. **Galgano F, Suzzi G, Favati F, Caruso M, Martuscelli M, Gardini F, Salzano G.** 2001. Biogenic amines during ripening in semicotto caprino cheese: role of enterococci. Int. J. Food Sci. Technol. **36:**153–160.
17. **González de Llano D, Cuesta P, Rodríguez A.** 1998. Biogenic amine production by wild lactococcal and leuconostoc strains. Lett. Appl. Microbiol. **26:**270–274.
18. **Pessione E, Pessione A, Lamberti C, Coisson DJ, Riedel K, Mazzoli R, Giunta C.** 2009. First evidence of a membrane-bound, tyramine and β-phenylethylamine producing tyrosine decarboxylase in *Enterococcus faecalis*: a two-dimensional electrophoresis proteomic study. Proteomics **9:**2695–2710.
19. **Kurtis CRP, Knowles PF, Parsons MR, Gaule TG, Phillips SEV, McPherson MJ.** 2011. Tyrosine 381 in *E. coli* copper amine oxidase influences substrate specificity. J. Neural Transm. **118:**1043–1053.
20. **Parrott S, Jones S, Cooper RA.** 1987. 2-Phenylethylamine catabolism of *Escherichia coli* K12. J. Gen. Microbiol. **133:**347–351.
21. **Ferrández A, Miñambres B, García B, Olivera ER, Luengo JM, García JL, Díaz E.** 1998. Catabolism of phenylacetic acid in *Escherichia coli*. Characterization of a new aerobic hybrid pathway. J. Biol. Chem. **273:**25974–25986.
22. **Teufel R, Mascaraque V, Ismail W, Voss M, Perera J, Eisenreich W, Haehnel W, Fuchs G.** 2010. Bacterial phenylalanine and phenylacetate catabolic pathway revealed. Proc. Natl. Acad. Sci. U. S. A. **107:**14390–14395.
23. **Ferrández A, García JL, Díaz E.** 2000. Transcriptional regulation of the divergent *paa* catabolic operons for phenylacetic acid degradation in *Escherichia coli*. J. Biol. Chem. **275:**12214–12222.
24. **Fic E, Bonarek P, Gorecki A, Kedracka-Krok S, Mikolajczak J, Polit A, Wasylewski Z.** 2009. cAMP receptor protein from *Escherichia coli* as a model of signal transduction in proteins–a review. J. Mol. Microbiol. Biotechnol. **17:**1–11.
25. **Azakami H, Yamashita M, Roh J, Suzuki H, Kumagai H, Murooka Y.** 1994. Nucleotide sequence of the gene for monoamine oxidase (*maoA*) from *Escherichia coli*. J. Ferment. Bioeng. **77:**315–319.
26. **Storz G, Imlay JA.** 1999. Oxidative stress. Curr. Opin. Microbiol. **2:**188–194.
27. **Christman MF, Storz G, Ames BN.** 1989. OxyR, a positive regulator of hydrogen peroxide-inducible genes in *Escherichia coli* and *Salmonella typhimurium*, is homologous to a family of bacterial regulatory proteins. Proc. Natl. Acad. Sci. U. S. A. **86:**3484–3488.
28. **Jacobson FS, Morgan RW, Christman MF, Ames BN.** 1989. An alkyl hydroperoxide reductase from *Salmonella typhimurium* involved in the defense of DNA against oxidative damage. Purification and properties. J. Biol. Chem. **264:**1488–1496.
29. **Altuvia S, Almiron M, Huisman G, Kolter R, Storz G.** 1994. The *dps* promoter is activated by OxyR during growth and by IHF and sigma S in stationary phase. Mol. Microbiol. **13:**265–272.
30. **Anjem A, Varghese S, Imlay JA.** 2009. Manganese import is a key element of the OxyR response to hydrogen peroxide in *Escherichia coli*. Mol. Microbiol. **72:**844–858.
31. **Liu Y, Bauer SC, Imlay JA.** 2011. The YaaA protein of the *Escherichia coli* OxyR regulon lessens hydrogen peroxide toxicity by diminishing the amount of intracellular unincorporated iron. J. Bacteriol. **193:**2186–2196.
32. **Jang S, Imlay JA.** 2010. Hydrogen peroxide inactivates the *Escherichia coli* Isc iron-sulphur assembly system, and OxyR induces the Suf system to compensate. Mol. Microbiol. **78:**1448–1467.
33. **Miller JH.** 1972. Experiments in molecular genetics. Cold Spring Harbor Laboratory Press, Cold Spring Harbor, NY.

34. **Datsenko KA, Wanner BL.** 2000. One-step inactivation of chromosomal genes in *Escherichia coli* K-12 using PCR products. Proc. Natl. Acad. Sci. U. S. A. **97:**6640–6645.
35. **Haldimann A, Wanner BL.** 2001. Conditional-replication, integration, excision, and retrieval plasmid-host systems for gene structure-function studies of bacteria. J. Bacteriol. **183:**6384–6393.
36. **Kullik I, Stevens J, Toledano MB, Storz G.** 1995. Mutational analysis of the redox-sensitive transcriptional regulator OxyR: regions important for DNA binding and multimerization. J. Bacteriol. **177:**1285–1291.
37. **Weski J, Ehrmann M.** 2012. Genetic analysis of 15 protein folding factors and proteases of the *Escherichia coli* cell envelope. J. Bacteriol. **194:**3225–3233.
38. **Imlay JA, Fridovich I.** 1991. Assay of metabolic superoxide production in *Escherichia coli*. J. Biol. Chem. **266:**6957–6965.
39. **Oliver DB.** 1996. Periplasm. *In* Neidhardt FC, Curtiss R, III, Ingraham JL, Lin ECC, Low KB, Magasanik B, Reznikoff WS, Riley M, Schaechter M, Umbarger HE (ed), *Escherichia coli* and *Salmonella*: cellular and molecular biology, 2nd ed, vol 1. ASM Press, Washington, DC.
40. **Neidhardt FC, Ingraham JL, Schaechter M.** 1990. Physiology of the bacterial cell: a molecular approach. Sinauer Associates, Inc., Sunderland, MA.
41. **Beers RFJ, Sizer IW.** 1952. A spectrophotometric method for measuring the breakdown of hydrogen peroxide by catalase. J. Biol. Chem. **195:**133–140.
42. **Choi H, Kim S, Mukhopadhyay P, Cho S, Woo J, Storz G, Ryu S.** 2001. Structural basis of the redox switch in the OxyR transcription factor. Cell **105:**103–113.
43. **Aslund F, Zheng M, Beckwith J, Storz G.** 1999. Regulation of the OxyR transcriptional factor by hydrogen peroxide and the cellular thiol-disulfide status. Proc. Natl. Acad. Sci. U. S. A. **96:**6161–6165.
44. **Seaver LC, Imlay JA.** 2001. Hydrogen peroxide fluxes and compartmentalization inside growing *Escherichia coli*. J. Bacteriol. **183:**7182–7189.
45. **Grant RA, Filman DJ, Finkel SE, Kolter R, Hogle JM.** 1998. The crystal structure of Dps, a ferritin homolog that binds and protects DNA. Nat. Struct. Biol. **5:**294–303.
46. **Ilari A, Ceci P, Ferrari D, Rossi G, Chiancone E.** 2002. Iron incorporation into *E. coli* Dps gives rise to a ferritin-like microcrystalline core. J. Biol. Chem. **277:**37619–37623.
47. **Kehres DG, Janakiraman A, Slauch JM, Maguire ME.** 2002. Regulation of *Salmonella enterica* serovar Typhimurium *mntH* transcription by H_2O_2, Fe^{2+}, and Mn^{2+}. J. Bacteriol. **184:**3151–3158.
48. **Lee JH, Yeo WS, Roe JH.** 2004. Induction of the *sufA* operon encoding Fe-S assembly proteins by superoxide generators and hydrogen peroxide: involvement of OxyR, IHF and an unidentified oxidant-responsive factor. Mol. Microbiol. **51:**1745–1755.
49. **Imlay JA, Linn S.** 1986. Bimodal pattern of killing of DNA-repair-defective or anoxically grown *Escherichia coli* by hydrogen peroxide. J. Bacteriol. **166:**519–527.
50. **Hengge R.** 2009. Proteolysis of sigmaS (RpoS) and the general stress response in *Escherichia coli*. Res. Microbiol. **160:**667–676.
51. **Ruiz N, Silhavy TJ.** 2005. Sensing external stress: watchdogs of the *Escherichia coli* cell envelope. Curr. Opin. Microbiol. **8:**122–126.
52. **Depuydt M, Leonard SE, Vertommen D, Denoncin K, Morsomme P, Wahni K, Messens J, Carroll KS, Collet J-F.** 2009. A periplasmic reducing system protects single cysteine residues from oxidation. Science **236:**1109–1111.
53. **Wilmot CM, Murray JM, Alton G, Parsons MR, Convery MA, Blakeley V, Corner AS, Palcic MM, Knowles PF, McPherson MJ, Phillips SEV.** 1997. Catalytic mechanism of the quinoenzyme amine oxidase from *Escherichia coli*: exploring the reductive half-reaction. Biochemistry **36:**1608–1620.
54. **Macomber L, Imlay JA.** 2009. The iron-sulfur clusters of dehydratases are primary intracellular targets of copper toxicity. Proc. Natl. Acad. Sci. U. S. A. **106:**8344–8349.
55. **Fitzpatrick PF.** 2010. Oxidation of amines by flavoproteins. Arch. Biochem. Biophys. **493:**13–25.
56. **Winterbourn CC, Hampton MB, Livesey JH, Kettle AJ.** 2006. Modeling the reactions of superoxide and myeloperoxidase in the neutrophil phagosome. Implications for microbial killing. J. Biol. Chem. **281:**39860–39869.
57. **Nikaido H, Rosenberg EV.** 1981. Effect of solute size on diffusion rates through the transmembrane pores of the outer membrane of *Escherichia coli*. J. Gen. Physiol. **77:**121–135.
58. **Jacobs NJ, Jacobs JM.** 1978. Quinones as hydrogen carriers for a late step in anaerobic heme biosynthesis in *Escherichia coli*. Biochim. Biophys. Acta **544:**540–546.
59. **Wanders RJA, Waterham HR.** 2006. Biochemistry of mammalian peroxisomes revisited. Annu. Rev. Biochem. **75:**295–332.
60. **Kerfeld CA, Heinhorst S, Cannon GC.** 2010. Bacterial microcompartments. Annu. Rev. Microbiol. **64:**391–408.
61. **Winterbourn CC, Metodiewa D.** 1999. Reactivity of biologically important thiol compounds with superoxide and hydrogen peroxide. Free Radic. Biol. Med. **27:**322–328.
62. **Jaakkola K, Kaunismaki K, Tohka S, Yegutkin G, Vanttinen E, Havia T, Pelliniemi LJ, Virolainen M, Jalkanen S, Salmi M.** 1999. Human vascular adhesion protein-1 in smooth muscle cells. Am. J. Pathol. **155:**1953–1965.
63. **Hrycay E, Bandiera SM.** 2012. The monooxygenase, peroxidase, and peroxygenase properties of cytochrome P450. Arch. Biochem. Biophys. **522:**71–89.
64. **Yamashita M, Azakami H, Yokoro N, Roh JH, Suzuki H, Kumagai H, Murooka Y.** 1996. *maoB*, a gene that encodes a positive regulator of the monoamine oxidase gene (*maoA*) in *Escherichia coli*. J. Bacteriol. **178:**2941–2947.